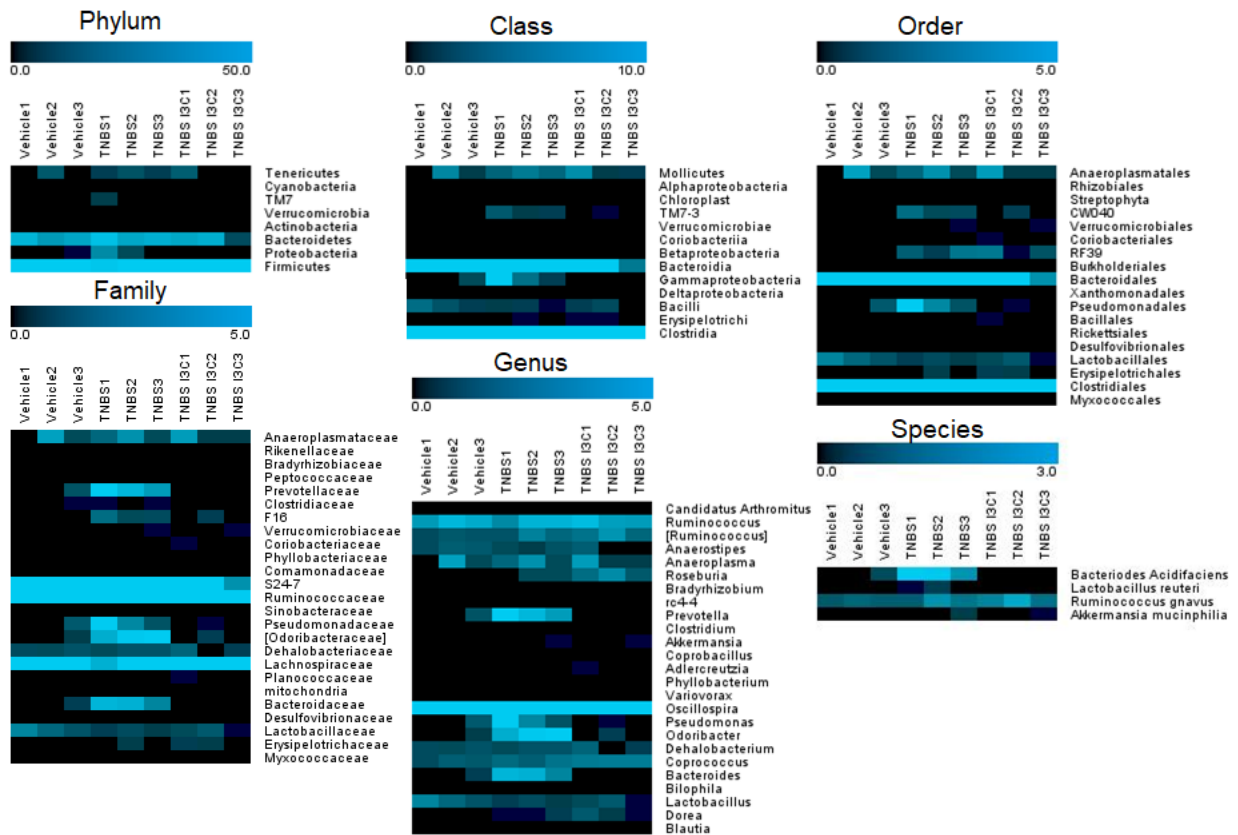
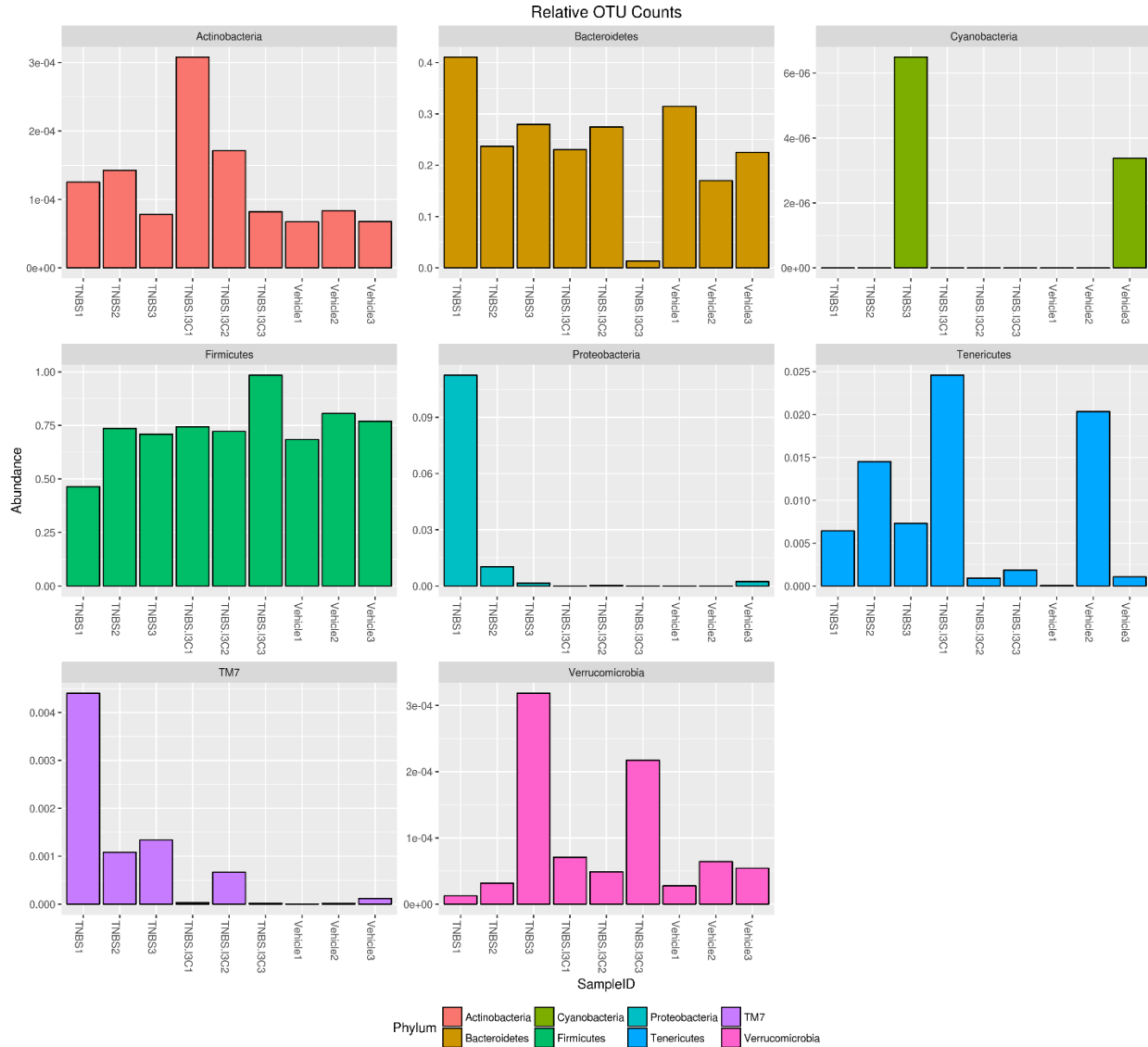


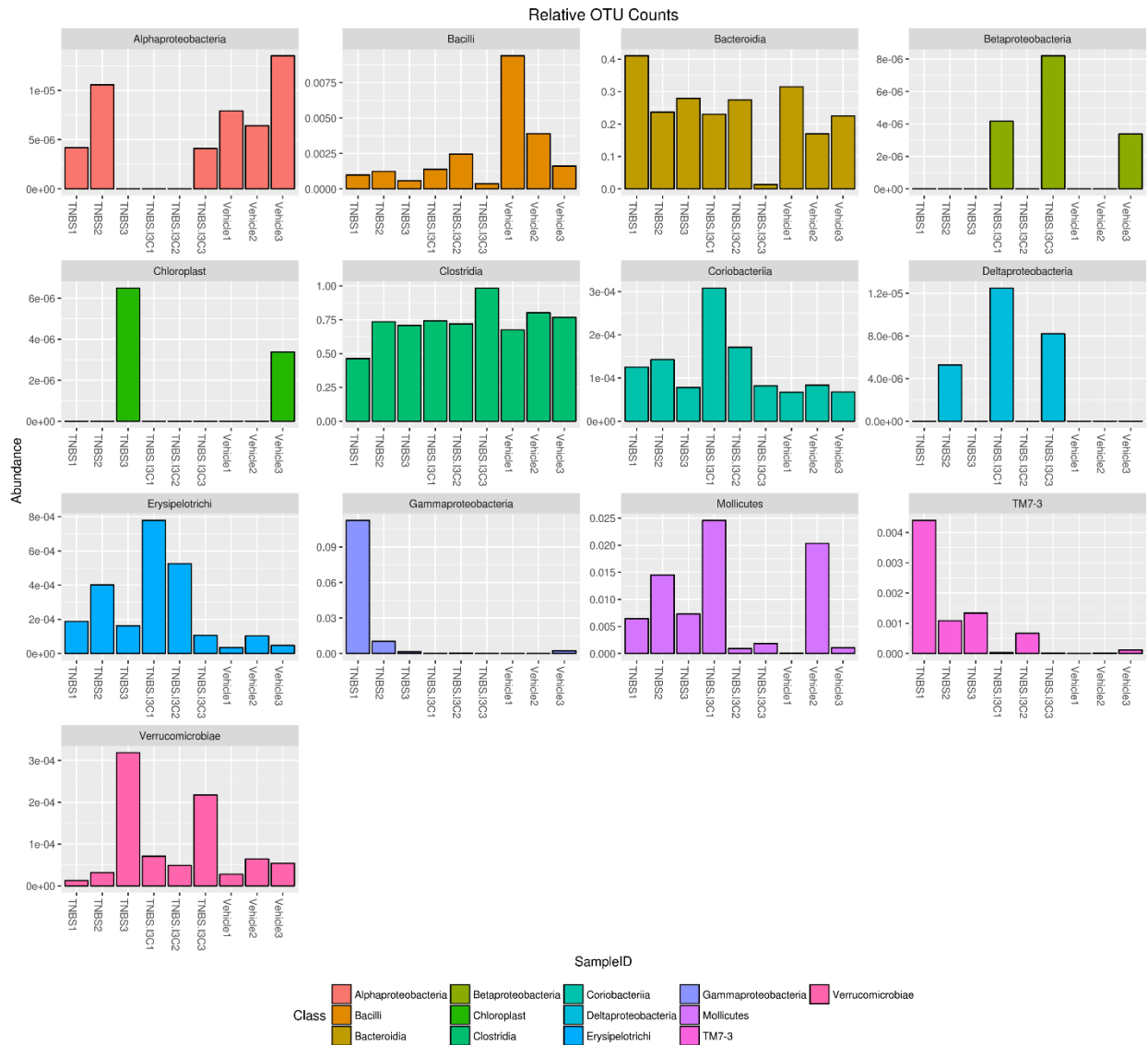
Supplemental Figure 1. Treatment with I3C resulted in amelioration of DSS-induced colitis. (A) DSS colitis was induced in female C57BL/6 mice to test the efficacy of treatment with I3C with the following experimental groups: Vehicle ($n=4$), I3C ($n=4$), DSS+Vehicle ($n=4$), DSS+I3C ($n=4$). Disease parameters assessed included percent weight loss (B), colon length (C), and macroscopic score (D). (E) On day 3, serum was also collected to determine the levels of circulating SAA. Error bars equal the SEM of representative data from at least 3 independent experiments. Statistical significance was determined with one-way ANOVA and Tukey's multiple comparisons test. * $P < 0.05$, ** $P < 0.01$, *** $P < 0.005$, **** $P < 0.001$.



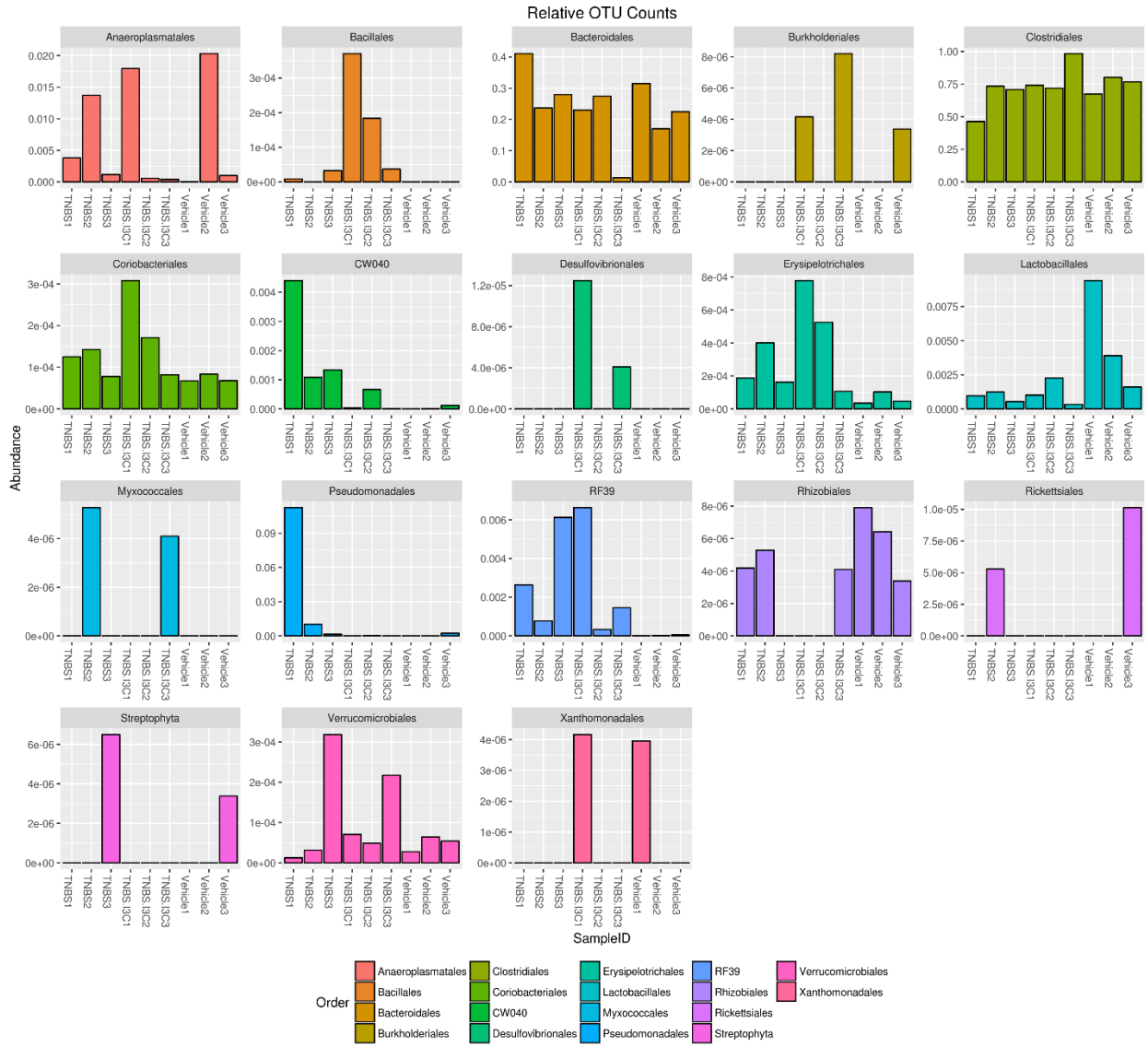
Supplemental Figure 2. Heatmap depicting percent OTU abundances at the phylum to species levels. Sequenced reads from colonic flushes of Vehicle (n=3), TNBS+Vehicle (n=3), and TNBS+I3C (n=3) were uploaded into the Nephele platform for 16S OTU analysis. Represented are heatmaps depicting percent OTUs with appropriate scale bars for each sample sequenced. Data are representative of one independent experiment.



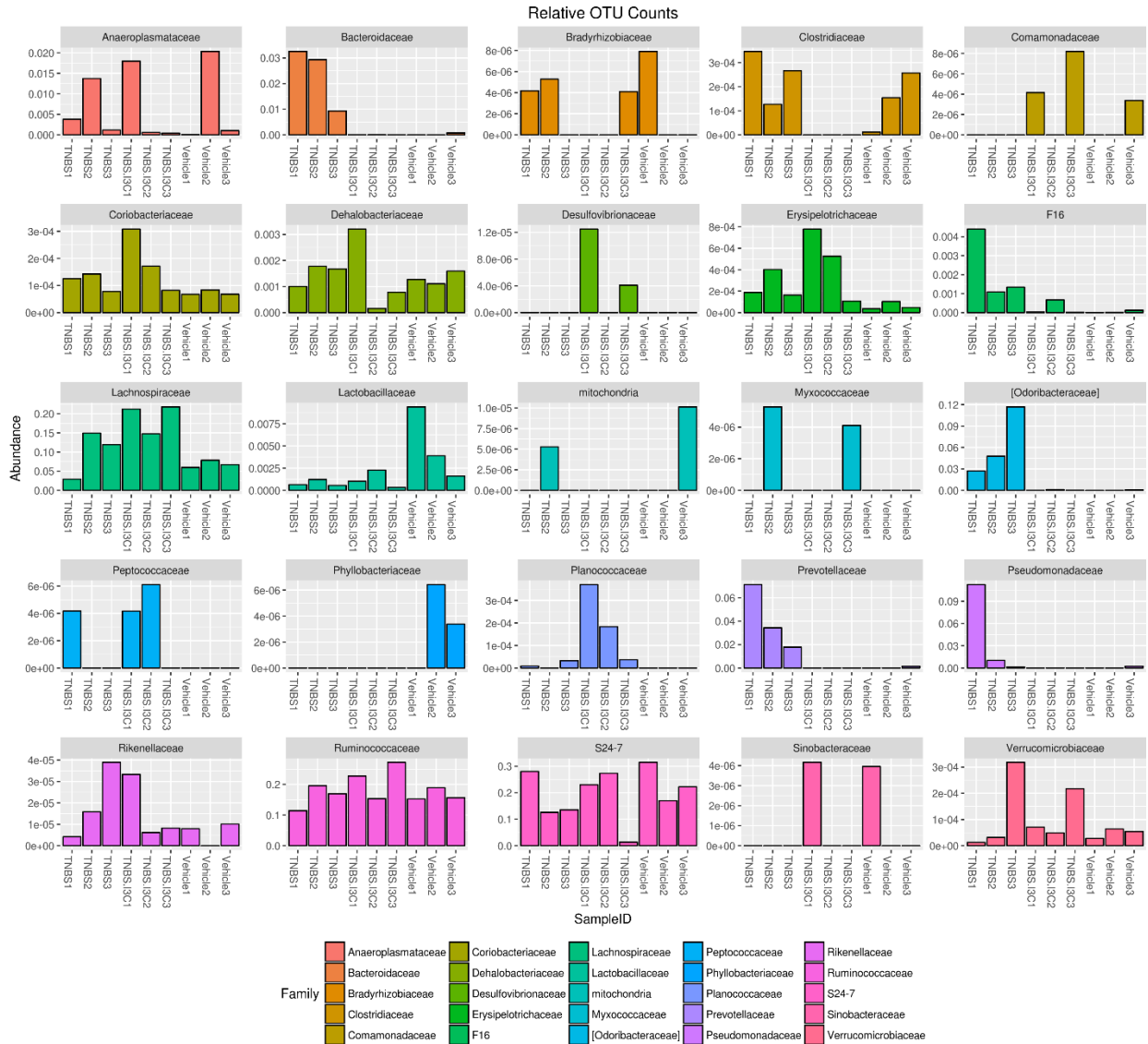
Supplemental Figure 3. Relative OTU abundances at the Phylum level. Sequenced reads from colonic flushes of Vehicle (n=3), TNBS+Vehicle (n=3), and TNBS+I3C (n=3) were uploaded into the Nephele platform for 16S OTU analysis. Individual sample bar graphs and figure legends were generated in the Nephele output files. Depicted are relative OTU counts. Data are representative of one independent experiment.



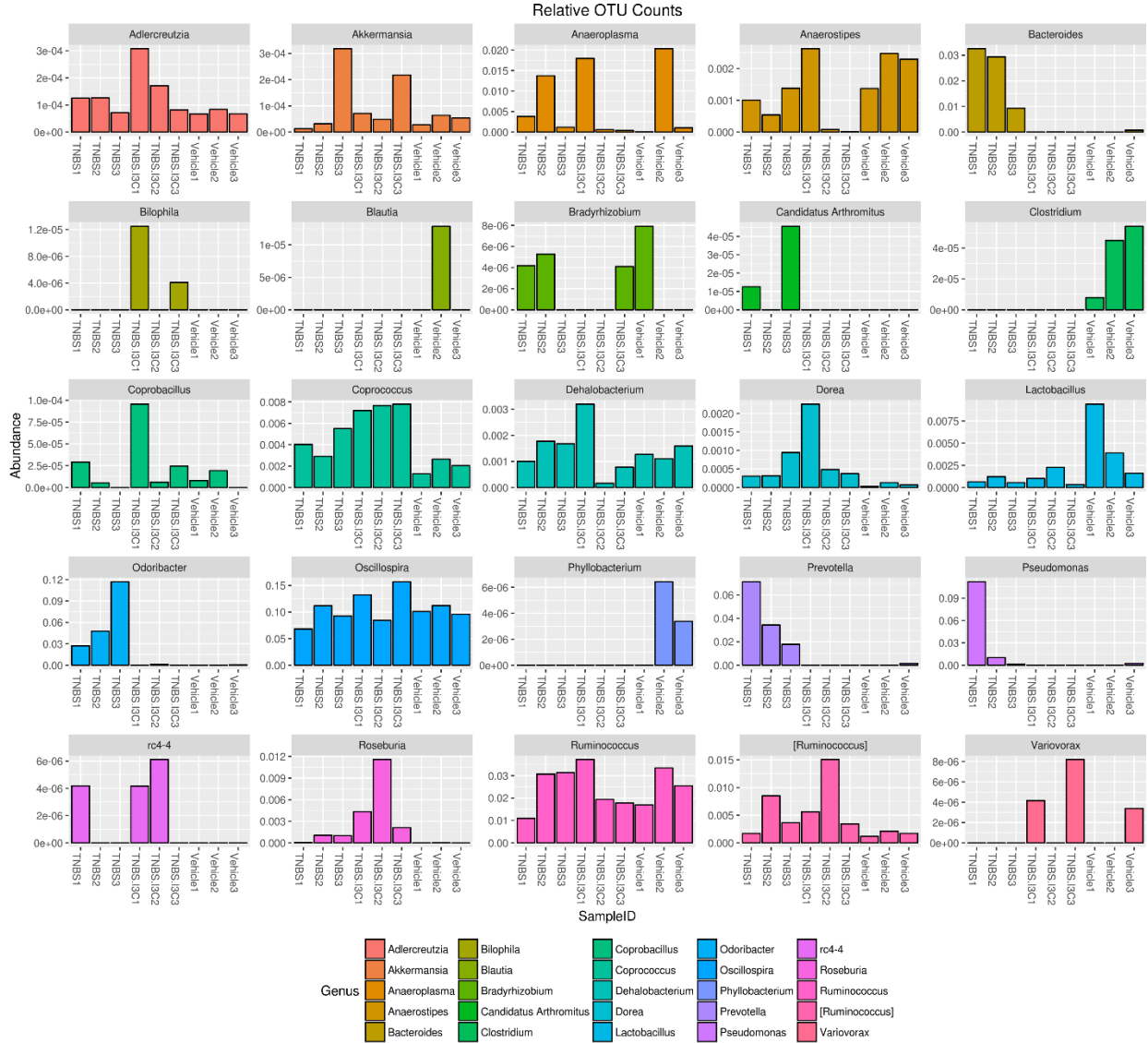
Supplemental Figure 4. Relative OTU abundances at the Class level. Sequenced reads from colonic flushes of Vehicle (n=3), TNBS+Vehicle (n=3), and TNBS+I3C (n=3) were uploaded into the Nephele platform for 16S OTU analysis. Individual sample bar graphs and figure legends were generated in the Nephele output files. Depicted are relative OTU counts. Data are representative of one independent experiment.



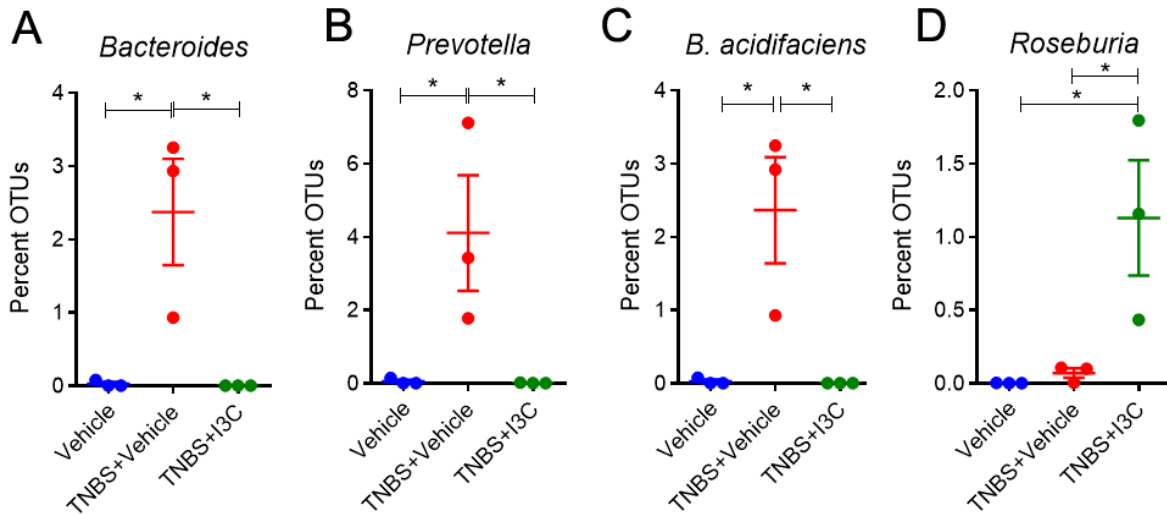
Supplemental Figure 5. Relative OTU abundances at the Order level. Sequenced reads from colonic flushes of Vehicle (n=3), TNBS+Vehicle (n=3), and TNBS+I3C (n=3) were uploaded into the Nephele platform for 16S OTU analysis. Individual sample bar graphs and figure legends were generated in the Nephele output files. Depicted are relative OTU counts. Data are representative of one independent experiment.



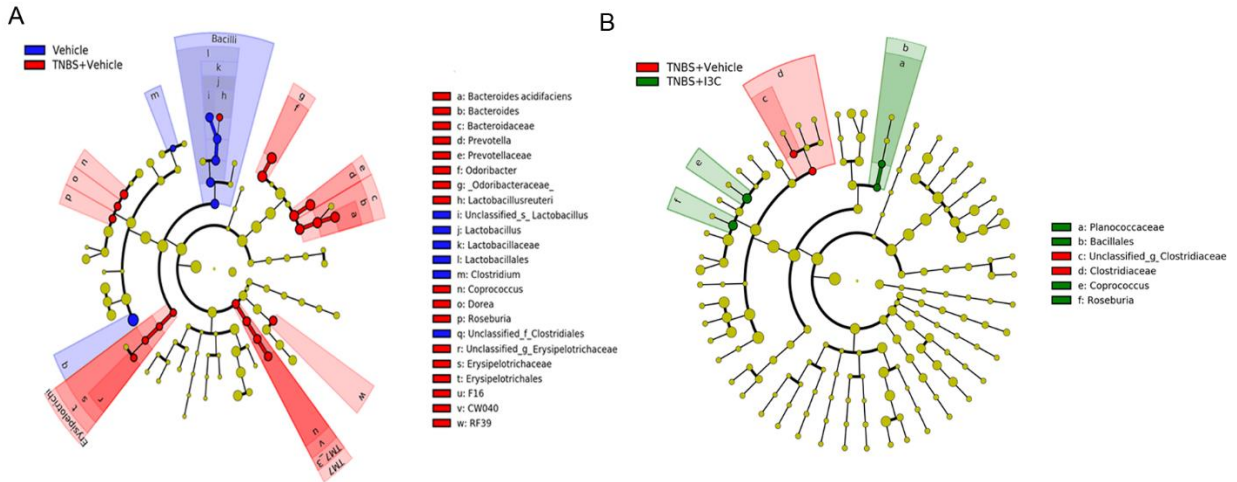
Supplemental Figure 6. Relative OTU abundances at the Family level. Sequenced reads from colonic flushes of Vehicle (n=3), TNBS+Vehicle (n=3), and TNBS+I3C (n=3) were uploaded into the Nephele platform for 16S OTU analysis. Individual sample bar graphs and figure legends were generated in the Nephele output files. Depicted are relative OTU counts. Data are representative of one independent experiment.



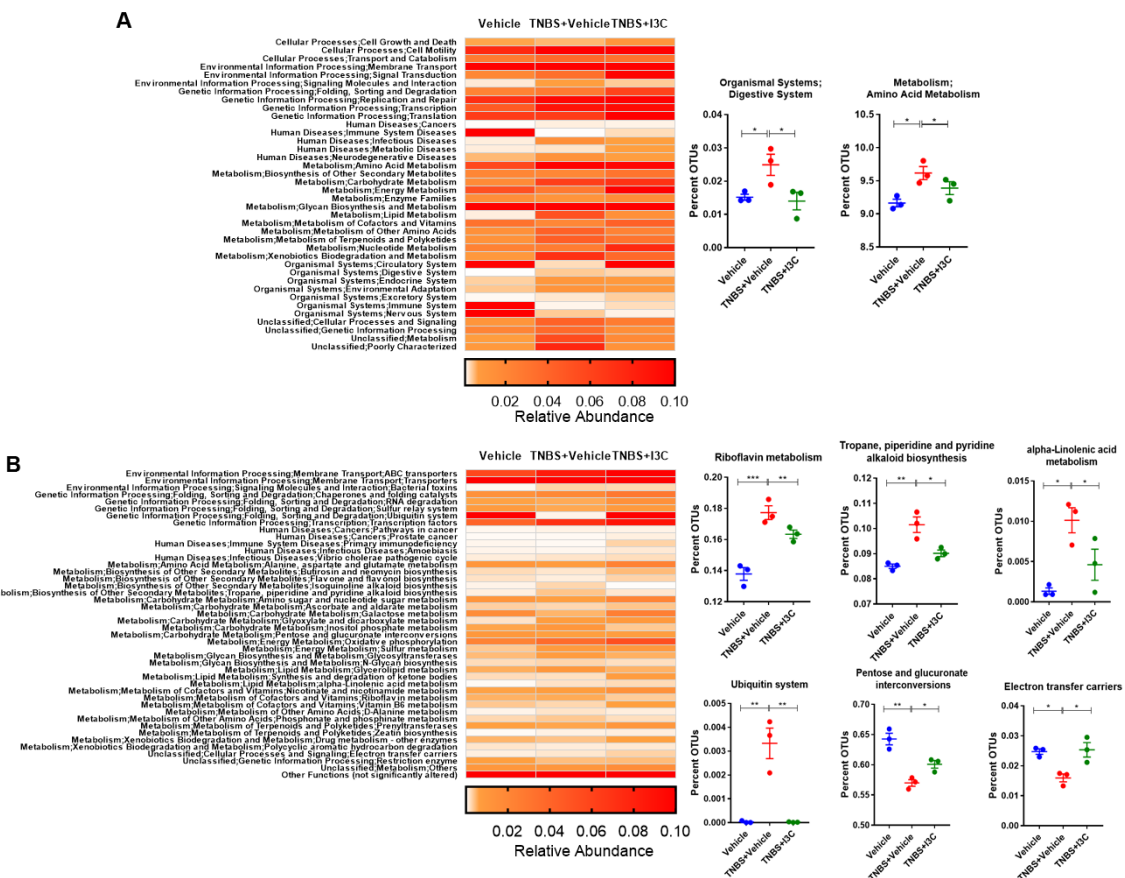
Supplemental Figure 7. Relative OTU abundances at the Genus level. Sequenced reads from colonic flushes of Vehicle (n=3), TNBS+Vehicle (n=3), and TNBS+I3C (n=3) were uploaded into the Nephel platform for 16S OTU analysis. Individual sample bar graphs and figure legends were generated in the Nephel output files. Depicted are relative OTU counts. Data are representative of one independent experiment.



Supplemental Figure 8. Significantly-altered OTU abundances at the genus and species level of I3C-treated TNBS colitis mice. 16S rRNA sequencing from the colonic flushes was performed on Vehicle (n=3), TNBS+Vehicle (n=3), and TNBS+I3C (n=3) experimental mice as depicted from one independent experiment. Sequenced reads were analyzed using the Nephel platform to determine abundance (%) of OTUs at the genus and species levels. Depicted are the significantly-altered OTUs at the genus and species level to include: *Bacteroides* (A), *Prevotella* (B), *B. acidifaciens* (C), and *Roseburia* (D). Error bars depict the SEM. One-way ANOVA with Tukey's multiple comparisons test was used to determine significance, * $P < 0.05$, ** $P < 0.01$, *** $P < 0.005$, **** $P < 0.001$.



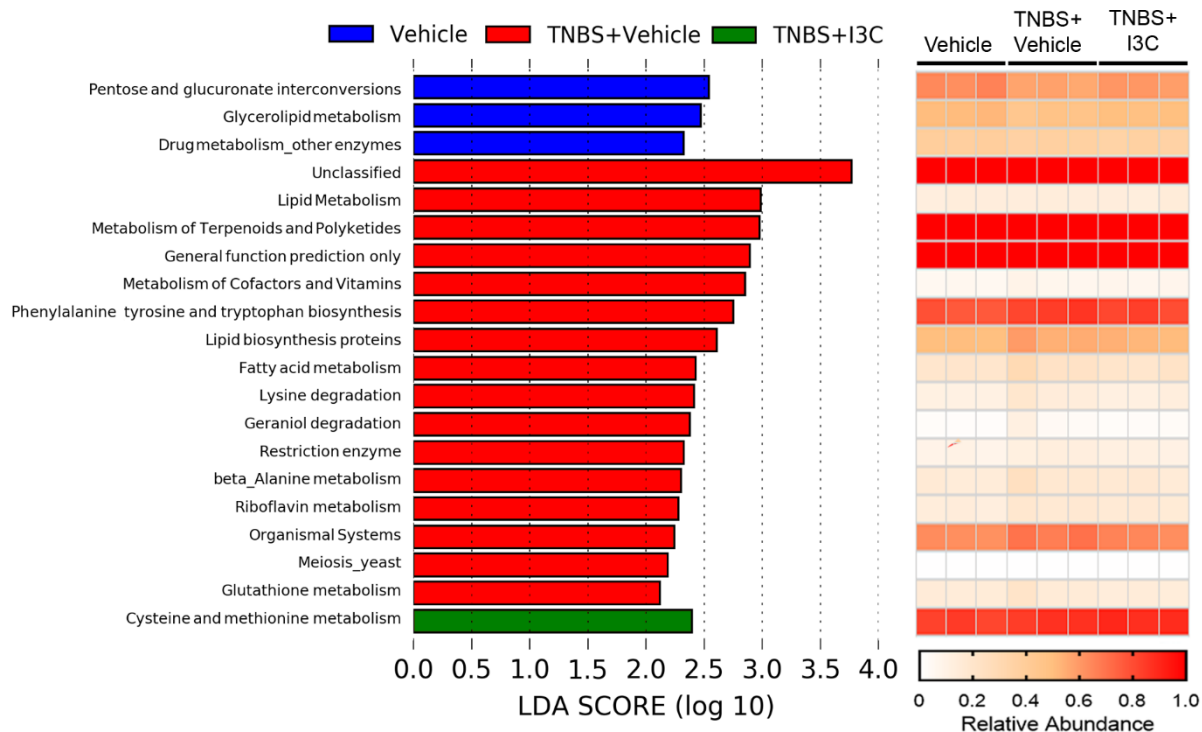
Supplemental Figure 9. Cladograms from LefSe analysis from colonic flushes. 16S rRNA sequencing from the colonic flushes was performed on Vehicle (n=3), TNBS+Vehicle (n=3), and TNBS+I3C (n=3) experimental mice and represent one independent experiment. The OTU-generated table from Nephel of sequenced reads was analyzed using LefSe. Depicted are cladograms generated from relative OTU comparisons between Vehicle versus TNBS+Vehicle (**A**), and TNBS+Vehicle versus TNBS+I3C (**B**). For LefSe data, the alpha factorial Kruskal-Wallis test among classes was set to 0.05, and the threshold on the logarithmic LDA score for discriminative features was set at 2. Data are representative of one independent experiment.



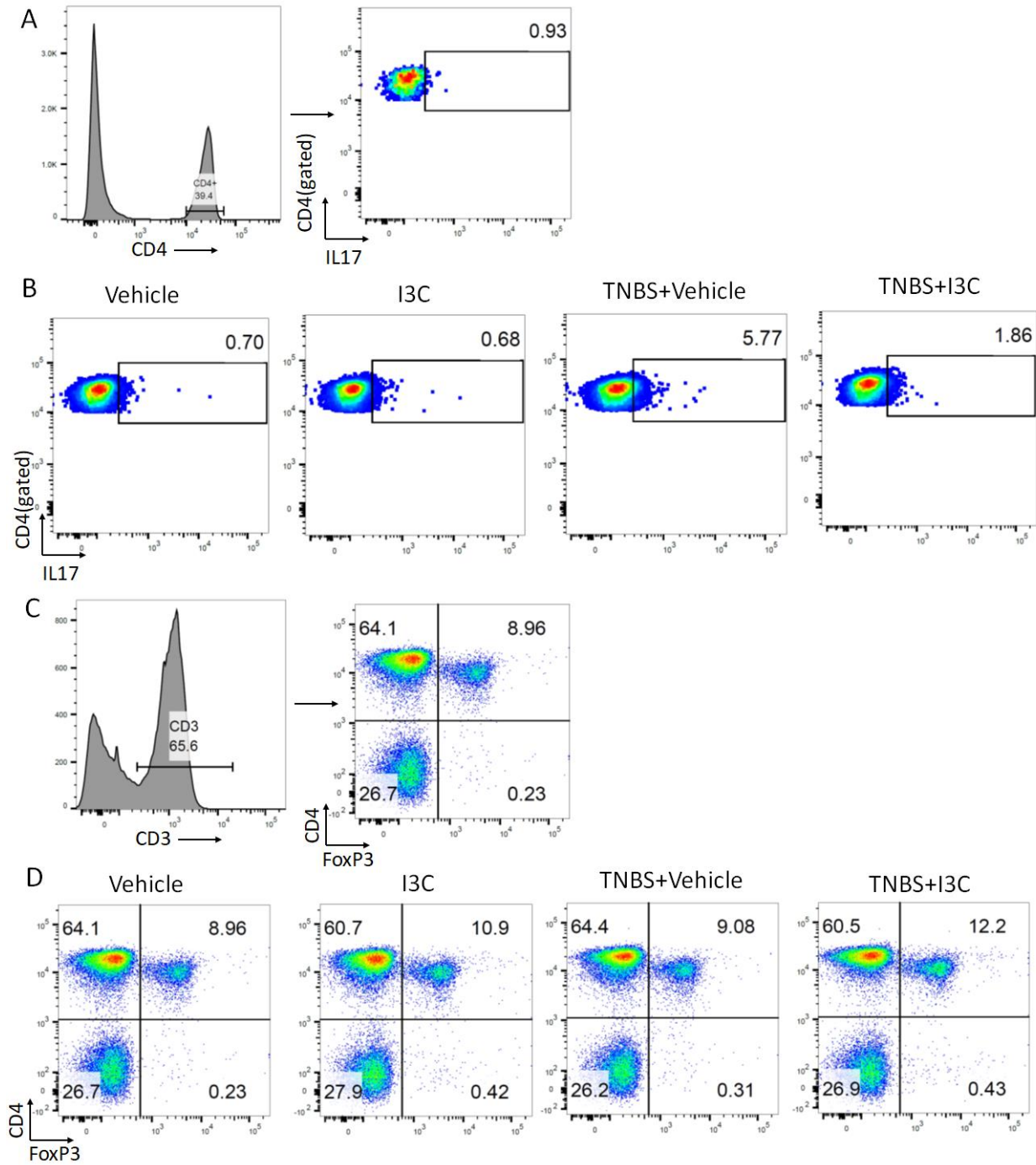
Supplemental Figure 10. L2 and L3 PiCRUST analysis of sequencing data.

Sequenced reads from colonic flushes of experimental mice (n=3 per group) were uploaded into the Nephel platform for analysis by PiCRUST. **(A)** The heatmap (left) depicts mean relative abundances attributed to the various L2 functions within the sampled data. Significantly altered KEGG pathways are depicted in the bar graphs to the right of the heatmap. **(B)** The heatmap (left) depicts mean relative abundances attributed to the various L3 functions within the sampled data. Significantly altered KEGG pathways are depicted in the bar graphs to the right of the heatmap. For bar graphs, each data point is the mean value \pm SEM. Data are representative of one independent experiment. One-way ANOVA with Tukey's multiple comparisons test was used to determine significance,

* $P < 0.05$, ** $P < 0.01$, *** $P < 0.005$, **** $P < 0.001$.



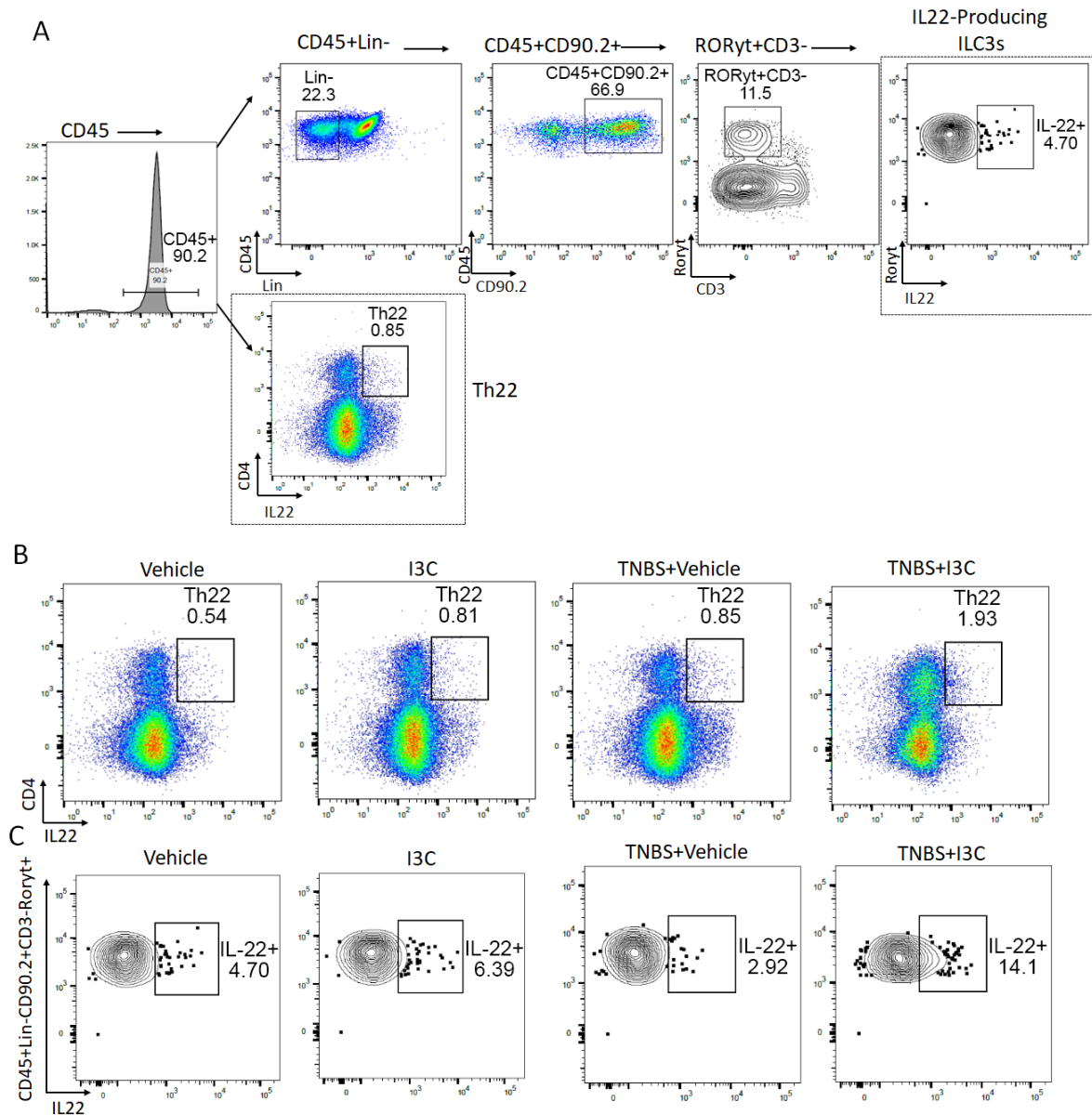
Supplemental Figure 11. LefSe analysis of L2 and L3 KEGG pathway using PiCRUSt. Sequenced reads from colonic flushes of experimental mice (n=3 per group) were uploaded into the Nephele platform for analysis by PiCRUSt. KEGG pathway tables generated from Nephele were analyzed using LefSe analysis. Depicted are the LDA scores (left) among the experimental groups, along with a corresponding heatmap (right) depicting relative abundances of the pathways. For LefSe data, the alpha factorial Kruskal-Wallis test among classes was set to 0.05, and the threshold on the logarithmic LDA score for discriminative features was set at 2. Data are representative of one independent experiment.



Supplemental Figure 12. Gating strategy for identifying Th17 and Tregs in the MLN.

Cells from the MLN from mice (Vehicle, n=5; I3C, n=5; TNBS+Vehicle, n=5; and TNBS+I3C, n=5) were isolated to determine total cell numbers for Th17 and Tregs. (A) Representative flow panel depicting the gating strategy for Th17 cells consisted of gating

on CD4+ cells (histogram) and those positive for IL17 (dot plot). **(B)** Representative flow panels depicting Th17 cells from each experimental group. **(C)** Representative flow panel depicting the gating strategy for Treg cells consisted of gating on CD3+ cells (histogram) and determining those double positive for CD4 and FoxP3 (dot plot). **(D)** Representative flow panels depicting Th17 cells from each experimental group. Gates were based on the use of negative controls (unstained cells) and positive controls (single-color antibody stains). Data are representative of at least four independent experiments.



Supplemental Figure 13. Gating strategy for identifying IL22-positive cells in the LP fraction. LP fraction from mice (Vehicle, n=5; I3C, n=5; TNBS+Vehicle, n=5; and TNBS+I3C, n=5) was isolated to determine total cell numbers for IL22+ cells. (A) Representative flow panels depicting the gating strategy for IL22+ Th cells consisted of gating on live CD45+ cells (histogram), then gating on CD4+IL22+ cells (dot plot). For IL22-producing ILC3s, gated CD45+ cells (histogram) were then gated on lineage

negative (Lin-) populations, followed by those that were CD90.2+, Roryt+, CD3-, and lastly IL22+. **(B)** Representative flow panels depicting Th22 cells from each experimental group. **(C)** Representative flow panels depicting IL22-producing ILC3 cells from each experimental group. Gates were based on the use of negative controls (unstained cells) and positive controls (single-color antibody stains). Data are representative of at least two independent experiments